Histol Histopathol (2025) 40: 711-720

Histology and Histopathology
From Cell Biology to Tissue Engineering

ORIGINAL ARTICLE Open Access

CRISPR-mediated WNK4 point mutation aggravates tumor progression and weakens chemotherapy sensitivity in gastric cancer

Xiaojun Ying[1], Zhen Ying[2], Xiaobing Gao[1], Yong Wang[3] and Xinting Lv[1]

[1]Department of General Surgery, [2]Department of Gynecology, Yongkang First People's Hospital, Yongkang City and [3]Department of General Surgery, Sir Run Run Shaw Hospital, Zhejiang University School of Medicine, Zhejiang Province, PR China

Summary. Objective. Gastric cancer (GC) is the fifth most common malignancy, the molecular targets of which have been increasingly explored in recent years. As a serine/threonine protein kinase, the role of WNK lysine deficient protein kinase 4 (WNK4) in GC was clarified in this study.

Methods. Human GC lines AGS and MKN45 were stably transfected with a WNK4 mutant constructed by the CRISPR/Cas9 method and treated with cis-dichlorodiammine platinum (CDDP, 2 μg/mL) and 5-fluorouracil (5-FU, 5 μg/mL) for 48h. Tumor-bearing mice were established with 5×10^6 mutant-type AGS cells, and injected with 40 mg/kg WP1066, the inhibitor of signal transducer and activator of transcription 3 (STAT3), for 21 days. Cell malignant potential and tumor growth were assessed. STAT3 activation was identified by western blot and immunohistochemistry. The interaction between WNK4 and STAT3 was determined using co-immunoprecipitation and immunofluorescence co-localization.

Results. WNK4 mutation promoted proliferation and invasion, and upregulated the p-STAT3/STAT3 value in GC cells with/without 5-FU and CDDP treatments, while inhibiting apoptosis of GC cells without drug treatment. In tumor-bearing mice, WNK4 mutation accelerated tumor growth, increased levels of p-STAT3, STAT3, and p-STAT3/STAT3, and strengthened the co-immunoprecipitation and co-localizing with STAT3; however, these effects were reversed by WP1066 treatment.

Conclusion. Through activating STAT3, WNK4 mutation impacts both the natural and drug-treated growth of GC cells or tumors, suggesting a new avenue for preclinical research.

Corresponding Author: Xinting Lv, Department of General Surgery, Yongkang First People's Hospital, 599 Jinshan West Road, Dongcheng Street, Yongkang City, Zhejiang Province, 321300, PR China. e-mail: lvxinting_lvx@163.com

www.hh.um.es. DOI: 10.14670/HH-18-810

Key words: WNK lysine deficient protein kinase 4, Mutation, Gastric cancer, Signal transducer and activator of transcription 3, CRISPR/Cas9

Introduction

Gastric cancer (GC) is the fifth most common malignancy, with around a 70% mortality rate in the world, as per the data of Global Cancer Statistics 2020 (Sung et al., 2021). The detrimental drivers of GC include age, high salt consumption, *Helicobacter pylori*, and low-vegetable and fruit-rich diets (Smyth et al., 2020). A population-based modeling study predicted that new cases and deaths of GC will increase to ~1.8 million and ~1.3 million, respectively, by 2040 (Morgan et al., 2022). So far, chemotherapy is still the pillar for those GC patients limited by surgical resection; however, the consequent chemoresistance challenges the survival of almost all cancer patients (including GC) (Zhang et al., 2022). Excitingly, targeted therapy is considered to hold promise for GC treatment and resistance alleviation (Patel and Cecchini, 2020).

In recent years, studies on molecular targets of GC have increased exponentially, involving a variety of molecules and pathways; for instance, circular RNAs (Zheng et al., 2023), autophagy-related gene CXCR4 (Zhao et al., 2023), the Hippo tumor suppressor pathway (Qiao et al., 2018), and the phosphatidyl-inositol 3-kinase (PI3K)/protein kinase B (AKT)/mammalian target of rapamycin (mTOR) signaling pathway (Kang and Chau, 2020). Protein kinase is implicated in various cellular functions, and its dysregulation is associated with different carcino-genesis processes (Kannaiyan and Mahadevan, 2018). In addition to AKT, several members of the serine/threonine protein family, such as kinase mitogen-activated protein kinase 1 (MAPK1) (Wang et al., 2023), calcium/calmodulin-dependent protein kinase kinase 2 (CAMKK2) (Najar et al., 2021), and

©The Author(s) 2024. **Open Access.** This article is licensed under a Creative Commons CC-BY International License.

serine/threonine-protein kinase 24 (STK24) (Chen et al., 2021), have been reported to play a promotive or inhibitory role in GC. The WNK lysine deficient protein kinase (WNK) family consists of four members and is a novel family of serine/threonine protein kinases that not only participates in ion transport across membranes, but is also connected to cancer-associated signaling networks, including PI3K/AKT and angiogenesis, which is a key factor in the development of cancer (Kankanamalage et al., 2018). WNK1 plays a positive role in angiogenesis and cancer metastasis, WNK3 inhibition induces antitumor immunity via repressing PD-L1 levels in tumor cells and motivating T cells (Hou et al., 2022; Yoon et al., 2022); WNK2 inactivation facilitates cancer progression (Xiu et al., 2022), hinting that the abnormal expressions of WNK family members impact cancer progression. WNK4, as the core of WNK, has been reported to cause pseudohypoaldosteronism type II and familial hyperkalemic hypertension, as a result of uncontrolled renal Na^+/Cl^- cotransporter due to WNK4 mutation-mediated abnormal expression (Murillo-de-Ozores et al., 2018; Rafael et al., 2018); nevertheless, no research focuses on the role of WNK4 mutation in cancer.

In this study, we adopted the clustered regularly interspaced short palindromic repeat (CRISPR)/associated nuclease 9 (Cas9) method to establish WNK4-mutation GC lines and tumor-bearing mice. Then, we investigated the mechanism underlying the biological function of WNK4 and its effects on different chemotherapeutic drug sensitivities in GC *in vivo* and *in vitro*. Our data suggested that WNK4 mutation exacerbated GC and diminished the sensitivity of GC cell lines to chemotherapeutic drugs via activating signal transducer and activator of transcription 3 (STAT3), hinting at WNK4 as a novel target for GC treatment.

Materials and methods

Ethics statement

All animal experiments in this study were conducted following the guidelines of the China Council on Animal Care and Use, and approved by the Ethics Committee of Zhejiang Baiyue Biotech Co., Ltd for Experimental Animals Welfare (ZJBYLA-IACUC-20230201).

Cell culture

Human GC cell lines AGS (CRL-1739, American Type Culture Collection, Rockefeller, Maryland, USA) and MKN45 (ACC-409, Deutsche Sammlung von Mikroorganismen und Zellkulturen, Brunswick, Germany) were seeded in 96-well plates containing Roswell Park Memorial Institute (RPMI)-1640 complete medium (PM150110B, Procell, Wuhan, China). Plates were kept in an incubator (51032874, ThermoFisher, Waltham, Massachusetts, USA) at 37°C and 5% CO_2.

Construction of cell lines with CRISPR/Cas9-induced WNK4 mutation

To mutate WNK4 in GC cell lines, single-stranded guide RNA (sgRNA) targeting exon 7 of WNK4 (5'-AGGCTGGATGGCACCCCCCC-3') was cloned into a pU6gRNACas9 vector (pGE-6, GenePharma, Shanghai, China). When cell confluence reached 70-80%, the vector was electroporated to GC cells (hereafter mutant-type (MUT)) with the CTS Xenon Electroporation System (A50301, ThermoFisher, USA) in an Invitrogen™ Neon™ Transfection System Instrument (MPK5000, ThermoFisher, USA). The wild-type (WT) GC cells acted as the negative control. After that, GC cells were grown in 96-well plates for a week until single-cell clones were obtained and frozen (Kabwe et al., 2022).

Genomic DNA sequencing

A mammalian genomic DNA extraction kit (D0061, Beyotime, Shanghai, China) was used to separate the genomic DNA of GC cells. Then, DNA templates and WNK4 primers (sense, 5'-AGTCACTTACCCTGCCTTCC-3', antisense, 5'-TGGATAGGGCAAAAGCCTGA-3') were mixed with PrimeSTAR® Max DNA Polymerase (R045A, Takara, Dalian, China) in the SimpliAmp™ Thermal Cycler (A24811, ThermoFisher, USA), followed by agarose gel electrophoresis. The target bands were collected and sequenced by Sangon Biotech (Shanghai, China) to confirm the mutation of target sequences.

Cell treatment

Cis-dichlorodiammine platinum (CDDP, 232120) and 5-fluorouracil (5-FU, 343922) were purchased from Sigma Aldrich (St. Louis, Missouri, USA). They were pre-dissolved in normal saline (S0817, Sigma Aldrich, USA) and diluted in RPMI-1640 medium to the final concentration of 2 μg/mL and 5 μg/mL, respectively. MUT and WT GC cells were cultured in the aforementioned mediums containing CDDP and 5-FU for 48h (Wang et al., 2020).

The 5-bromo-2-deoxyuridine (BrdU) enzyme-linked immunosorbent assay (ELISA)

The Cell Proliferation ELISA, BrdU (11669915001, Roche, Meylan, France) was utilized to assess the proliferation of GC cells, as described in a previous study (Zuo et al., 2018). In detail, GC cells were seeded in a 96-well plate at a density of 1×10^4 cells/well (100 μL). After 24h, 10 μL BrdU labeling solution was incubated with cells for another 6h, followed by the addition of FixDenat, Anti-BrdU-POD working solution, and Substrate Solution

in turn. Finally, the optical density (OD) value was measured in a Multiskan™ FC Microplate Photometer (51119180ET, ThermoFisher, USA).

Colony formation assay

GC cells (1×10^3 cells/well) were grown in 6-well plates for two weeks for colony formation. Then, 4% paraformaldehyde (PN4204, G-CLONE, Beijing, China) and Giemsa (G1010, Solarbio, Beijing, China) were used to fix and stain cells at room temperature. After cells were washed with phosphate-buffered solution (PBS, abs962, Absin, Shanghai, China), the colony formation rate was calculated as [the number of cell colonies (≥50 per colony)/total cell number] ×100% under a BX53F microscope (OLYMPUS, Tokyo, Japan).

Flow cytometry

Cell apoptosis was tested as per the instructions of the Annexin-V-FITC Apoptosis Detection Kit (C1062L, Beyotime, China). Briefly, 1×10^5 GC cells were suspended in Annexin V-FITC Conjugate solution (195 μL), and then incubated with Annexin V-FITC (5 μL) and Propidium iodide staining solution (10 μL) for 15 min at room temperature without light. Finally, the samples were analyzed with an Attune™ NxT Flow Cytometer (A24859, ThermoFisher, USA) at the excitation wavelength of 488 nm.

Transwell assay

GC cells (1×10^4 cells/well) in serum-free medium (100 μL) were transferred into the upper chamber of 6-well Transwell plates (8-μm pore filters, 140644, ThermoFisher, USA) precoated with Matrigel (E1270, Sigma Aldrich, USA), with the lower chamber containing 600 μL normal medium and 10% fetal bovine serum (S9020, Solarbio, China). Following a 48-h incubation, only cells invading the lower chamber were fixed with 4% paraformaldehyde and stained with crystal violet (G1063, Solarbio, China). Lastly, stained cells were observed under the BX53F microscope at ×250 magnification, and the invasion rate was calculated as [the number of invaded cells/total cell number] ×100%.

Subcutaneous tumor growth experiment

BALB/c athymic mice (6 weeks old, female, n=30) were adaptively fed for a week, and then divided into AGS-WT, AGS-MUT, and AGS-MUT+WP1066 groups (n=10/group). As required, mice were subcutaneously injected with 5×10^6 WT or MUT AGS cells, after which tumor size was measured thrice a week for 25 days and tumor volume was calculated with the formula $V= 0.5 \times Length \times Width^2$ (Wei et al., 2015). During this period, when tumors reached ~10 mm in length, mice in the AGS-MUT+WP1066 group were injected with 40 mg/kg STAT3 inhibitor (WP1066, 573097, Sigma Aldrich, USA) in dimethyl sulfoxide (DMSO, D1435, Sigma Aldrich, USA) once every 3 days for 21 days; mice in the AGS-MUT group only received DMSO as a control (Zhou et al., 2014). In the end, all mice were sacrificed by cervical dislocation after intraperitoneal injection with 150 mg/kg of sodium pentobarbital (P3761, Haoran Biological Technology, Shanghai, China), and tumors were separated and weighed.

Immunohistochemistry

The tumors were sliced into 6-μm paraffin sections following fixation, permeation, and dehydration for immunohistochemical staining. Next, sections post-rehydration were soaked in PBS including Triton X-100 (T8787, Sigma Aldrich, USA) and 30% H_2O_2 (323381, Sigma Aldrich, USA) for 30 min without light at room temperature. Sections were treated with antigen repair buffer (C1031, Solarbio, China) at 37°C for 20 min, immersed in 5% goat serum (SL038, Solarbio, China) for 30 min at room temperature, and incubated with primary antibodies against STAT3 (ab68153, Abcam, Cambridge, UK) and p-STAT3 (ab267373, Abcam, UK) overnight at 4°C. Then, the horseradish peroxidase-conjugated IgG (ab97051, Abcam, UK) was used to incubate sections for 30 min at 37°C. The DAB Horseradish Peroxidase Color Development Kit (P0203, Beyotime, China) was used to color sections. After sealing, sections were observed using a BX53F microscope at ×100 magnification.

Co-immunoprecipitation

An Immunoprecipitation Kit with Protein G Magnetic Beads (P2177S, Beyotime, China) was used to verify the connection between WNK4 and STAT3. Small pieces of tumors were mixed with Lysis Buffer with Protease Inhibitor Cocktail and fully ground. After full lysis, the lysate supernatant was collected following centrifugation, and incubated with Protein G magnetic beads adsorbed with anti-STAT3 (ab32500, Abcam, UK) and control IgG (A7001, Beyotime, China) for 2h at room temperature. Finally, the beads were separated and heated in sodium dodecyl sulfate-polyacrylamide gel electrophoresis (SDS-PAGE) Sample loading buffer (1×) was added at 95°C for 5 min, and the supernatant was collected for a western blot assay (Arreola-Peralta et al., 2018).

Immunofluorescence co-localization

The paraffin-embedded tumor sections were permeabilized with 0.1% Triton X-100 and non-specific binding was blocked with 1% Bovine Serum Albumin (V900933, Sigma Aldrich, USA). Then, Alexa Fluor® 647-coupled WNK4 antibody (ab311130, Abcam, UK) and Alexa Fluor® 488-coupled STAT3 (ab214632, Abcam, UK) were incubated with sections overnight at 4°C without light. Finally, sections were counterstained

with diamidinyl-2-phenylindole (D9542, Sigma Aldrich, USA) prior to observation under a fluorescence confocal microscope (IX71, OLYMPUS, Japan) at ×400 magnification (Yu et al., 2015).

Western blot

RIPA Buffer (R0010, Solarbio, China) was employed to extract proteins from GC cells and tumors. Following a 5-minute boiling water bath, the protein concentration was determined by the BCA Protein Assay Kit (PC0020, Solarbio, China). Via SDS-PAGE, proteins were separated in NuPAGE™ 4-12%, Bis-Tris (NP0321BOX, ThermoFisher, USA). The Immobilon-P polyvinylidene fluoride (PVDF) membrane (YA1701, Solarbio, China) was loaded with separated proteins and blocked with Blocking Buffer (37581, ThermoFisher, USA) for 1h at room temperature. Then, the membrane was incubated with primary antibodies at 4ºC overnight, and secondary antibodies for 1h at room temperature. At last, following the Band-Now Pre-Staining Protein Sample Treatment Buffer for SDS-PAGE (P1050, Solarbio, China) treatment, the band signals were analyzed on a 5200 imaging system (Tanon, Shanghai, China). Data analysis was achieved with the help of Image J software (1.52s version, National Institutes of Health, Bethesda, Maryland, USA), with GAPDH as an internal reference.

The antibodies used, from Cell Signaling Technology (Beverly, Massachusetts, USA), were the following: primary antibodies including p-STAT3 (#9145, 79/86 kDa, 1:2000), STAT3 (#9139, 79/86 kDa, 1:1000), WNK4 (#5713S, 130 kDa, 1:1000), and GAPDH (#5174, 37 kDa, 1:1000), and secondary antibodies including anti-rabbit IgG (#7074, 1:1000) and anti-mouse IgG (#7076, 1:1000).

Statistical analyses

All data in this study were obtained from assays independently repeated three times and expressed as mean ± standard deviation by GraphPad Prism 8 (GraphPad, Inc., La Jolla, California, USA). Data between two groups in Figure 1B-K were analyzed by independent samples *t*-test, and those among multiple groups were dissected by one-way analysis of variance. The statistical significance was defined when the *p*-value was below the threshold of 0.05.

Results

WNK4 mutation promoted the malignant potential of GC cells in vitro

Using the CRISPR/Cas9 method, a single nucleotide, guanine, was deleted at position 1816 of the *WNK4* gene, as shown in Figure 1A. The WT and MUT of WNK4 were electroporated into AGS and MKN45 cells to explore the role of WNK4 in GC cells. By the BrdU ELISA (Fig. 1B,C) and colony formation assay (Fig. 1D,E), the OD value and relative colony formation rate of AGS and MKN45 cells were proven to be higher in the MUT group than in the WT group ($p<0.01$), hinting that WNK4 mutation promoted the proliferation of GC cells. Subsequent results from flow cytometry (Fig. 1F,G) and Transwell assay (Fig. 1H,I) suggested that WNK4 mutation diminished the apoptosis of AGS and MKN45 cells and elevated invasive cells ($p<0.001$). Considering the crucial role of STAT3 in GC development, we herein quantified the protein expression levels of p-STAT3 and STAT3, and found upregulation of p-STAT3/STAT3 following WNK4 mutation in AGS and MKN45 cells (Fig. 1J,K, $p<0.05$), indicating the activation of STAT3.

WNK4 mutation led to the decreased drug sensitivity of GC cells

As known to all, the chemoresistance to 5-FU and CDDP is a huge problem in cancer treatment. In order to explore the effects of WNK4 on GC cell sensitivity to these drugs, 5 μg/mL 5-FU and 2 μg/mL CDDP were utilized to treat WT and MUT AGS and MKN45 cells. Data from the BrdU ELISA (Fig. 2A,B) and colony formation assay (Fig. 2C-E) exhibited that the OD value and colony formation rate of AGS and MKN45 cells were increased in the MUT+5-FU and MUT+CDDP groups relative to WT+5-FU and WT+CDDP groups ($p<0.01$, MUT+5-FU vs. WT+5-FU; MUT+CDDP vs. WT+CDDP), suggesting the promoting role of WNK4 mutation in the proliferation of drug-treated GC cells. Also, the quantification of p-STAT3 and STAT3 revealed that WNK4 mutation enhanced STAT3 activation in drug-treated GC cells, as evidenced by the upregulation of p-STAT3/STAT3 in 5-FU/CDDP-treated AGS and MKN45 cells (Fig. 2F-I, $p<0.01$). These findings illustrated that WNK4 mutation lowered the sensitivity of GC cells to 5-FU and CDDP.

STAT3 inhibitor reversed the effects of WNK4 mutation on accelerating tumor growth and activating STAT3 in tumor-bearing mice

In order to explore the interaction between WNK4 and STAT3 in GC, tumor-bearing mice were constructed with WT or MUT AGS cells, and some mice were injected with STAT3 inhibitor WP1066. In line with Figure 3A,B, the tumor volume of mice within 25 days and their final tumor weight in the AGS-MUT group were significantly elevated in comparison with the AGS-WT group ($p<0.01$), while those in the AGS-MUT+WP1066 group were reduced compared with AGS-MUT group ($p<0.001$), suggesting that STAT3 inhibitor reversed the effects of WNK4 mutation on accelerating tumor growth.

In addition, the results from immunohistochemistry (Fig. 3C) and western blot (Fig. 3D-G) demonstrated that WNK4 mutation enhanced the expression of p-

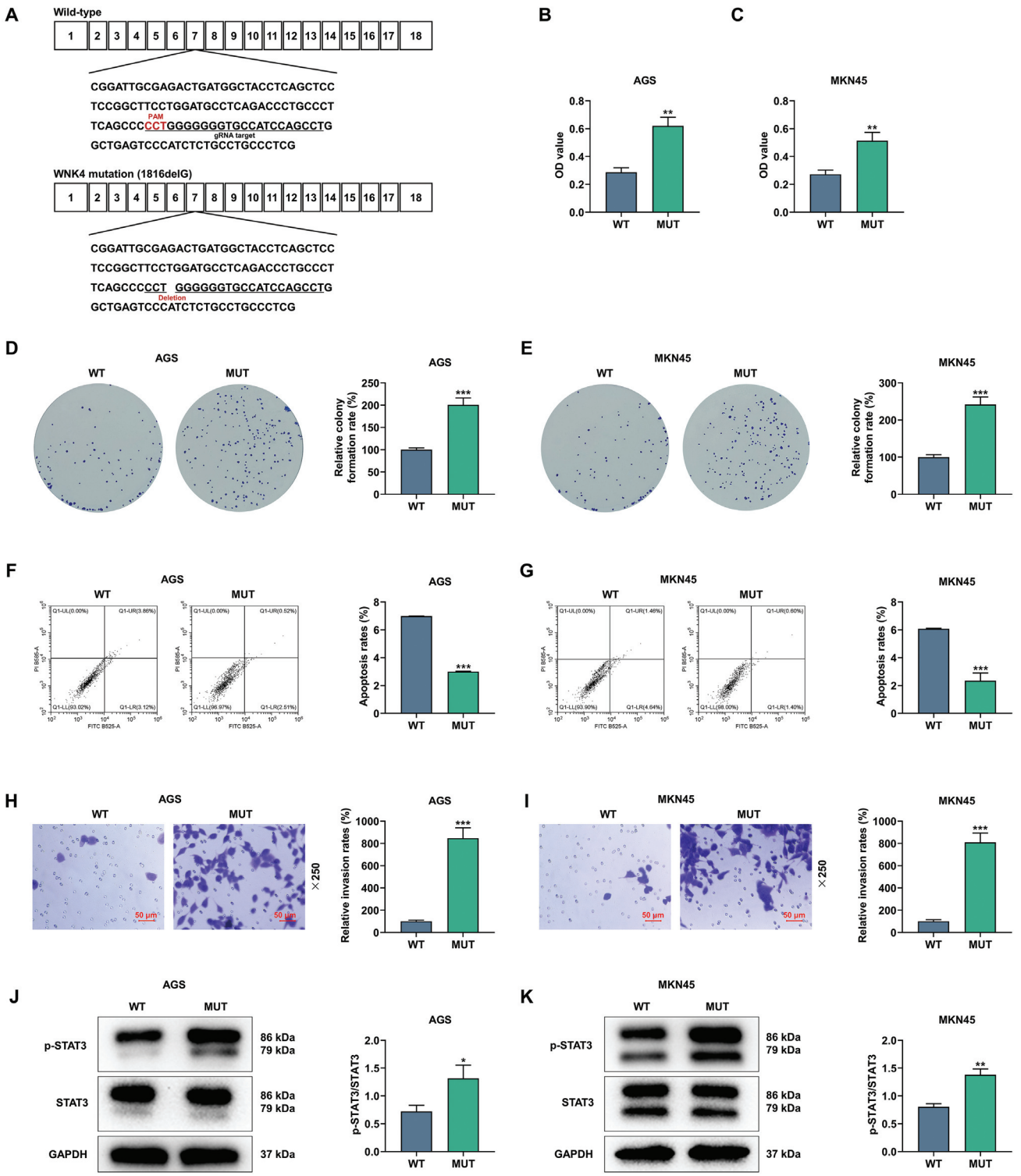

Fig. 1. WNK4 mutation promoted the malignant progression of GC cells *in vitro*. **A.** Schematic representation of the CRISPR-mediated mutations of exons 7 in *WNK4* (c.1816delG). **B, C.** BrdU ELISA was conducted to test the proliferation of AGS and MKN45 cells. **D, E.** A colony formation assay was performed to evaluate the proliferation of AGS and MKN45 cells. **F, G.** Flow cytometry was employed to determine the apoptosis of AGS and MKN45 cells. **H, I.** A Transwell assay was used to measure the invasion of AGS and MKN45 cells. **J, K.** Protein levels of p-STAT3 and STAT3 in AGS and MKN45 cells were measured by western blot, with GAPDH as the internal reference. *p<0.05, **p<0.01, ***p<0.001 vs. WT. WNK4, WNK lysine deficient protein kinase 4; GC, gastric cancer; CRISPR, clustered regularly interspaced short palindromic repeat; gRNA, guide RNA; BrdU, 5-bromo-2-deoxyuridine; ELISA, enzyme-linked immunosorbent assay; STAT3, signal transducer and activator of transcription 3; p-STAT3, phosphorylated STAT3; OD: optical density; WT, wild-type; MUT, mutant-type.

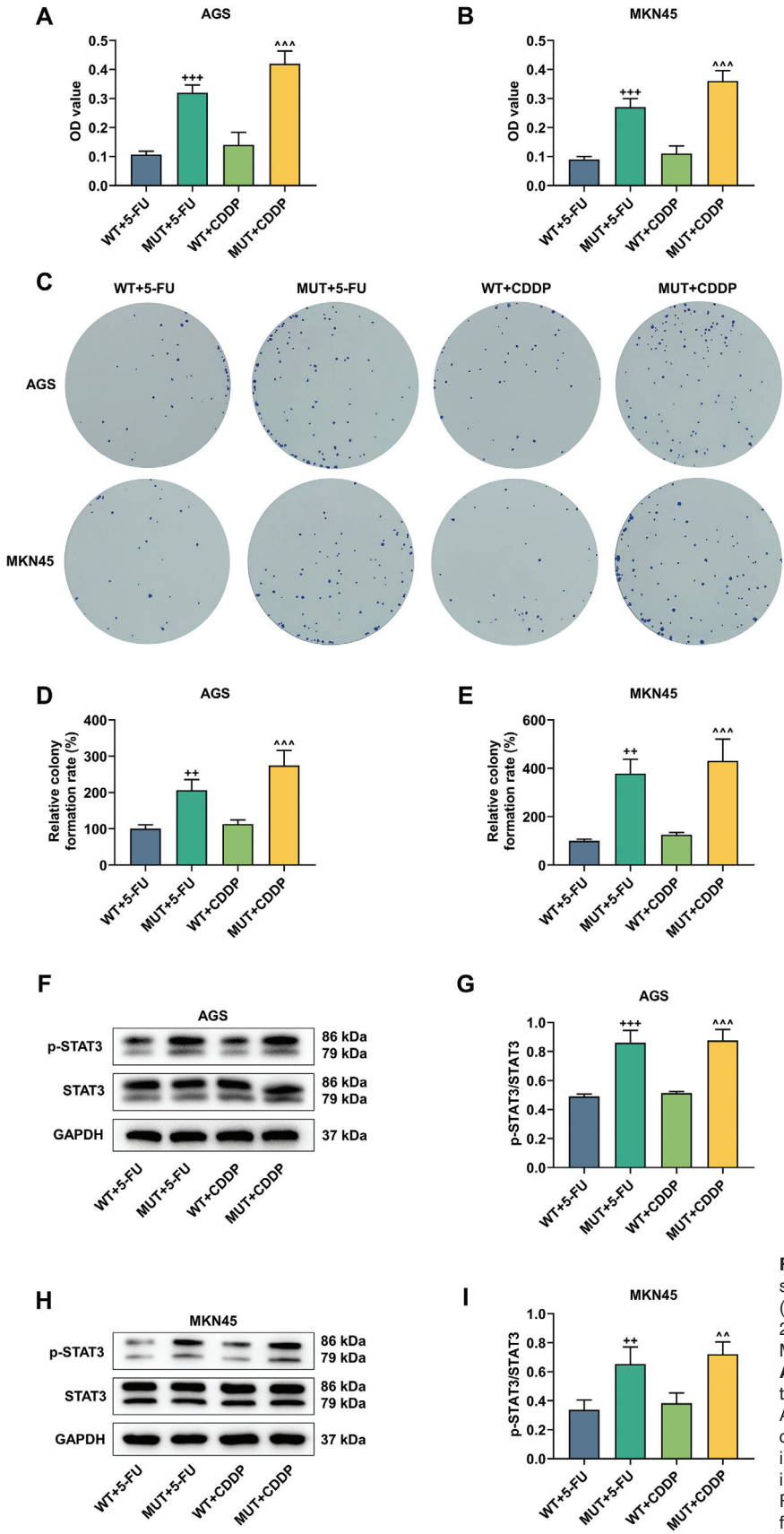

Fig. 2. WNK4 mutation led to the decrease in drug sensitivity of GC cells. **A-I.** AGS and MKN45 cells (WT and MUT) were treated with 5 μg/mL 5-FU and 2 μg/mL CDDP for 48h, respectively (WT+5-FU, MUT+5-FU, WT+CDDP, and MUT+CDDP groups). **A, B.** The proliferation of GC cells was evaluated through BrdU ELISA. **C-E.** The colony formation in AGS and MKN45 cells. **F-I.** Western blot data displayed the expressions of p-STAT3 and STAT3 in AGS and MKN45 cells, with GAPDH as the internal reference. $^{++}p<0.01$, $^{+++}p<0.001$, vs. WT+5-FU, $^{\wedge\wedge}p<0.01$, $^{\wedge\wedge\wedge}p<0.001$, vs. WT+CDDP. 5-FU, 5-fluorouracil; CDDP, Cis-dichlorodiammine-platinum.

STAT3 and STAT3 and the value of p-STAT3/STAT3 in tumors ($p<0.01$), while STAT3 inhibitor reversed the upregulation of p-STAT3 and STAT3 ($p<0.001$). To further confirm the interaction between WNK4 and STAT3, a co-immunoprecipitation assay and immunofluorescence co-localization were carried out. It was observed that WNK4 mutation amplified the enrichment of WNK4, p-STAT3, and STAT3 in the pull-down STAT3 complexes in the co-immunoprecipitation assay (Fig. 3H) and extended the co-localization of WNK4 with STAT3 in both the cytoplasm and nucleus (Fig. 3I), which was counteracted by STAT3 inhibitor (Fig. 3H,I). The above results revealed that WNK4 mutation promoted the activation of STAT3 by the binding interaction.

Discussion

In the current study, we generated an unprecedented mutant WNK4. We proved that the GC cell lines and tumor-bearing mice harbored a WNK4 mutation with a monoallelic single deleted guanine nucleotide at position 1816 through the CRISPR/Cas9 genome editing method, which led to a remarkable functional imbalance in WNK4. Herein, WNK4 mutation potentiated the *in vitro* malignant potential of GC cells, maintained the proliferation of 5-FU/CDDP-treated GC cells, and promoted tumor growth in tumor-bearing mice, along

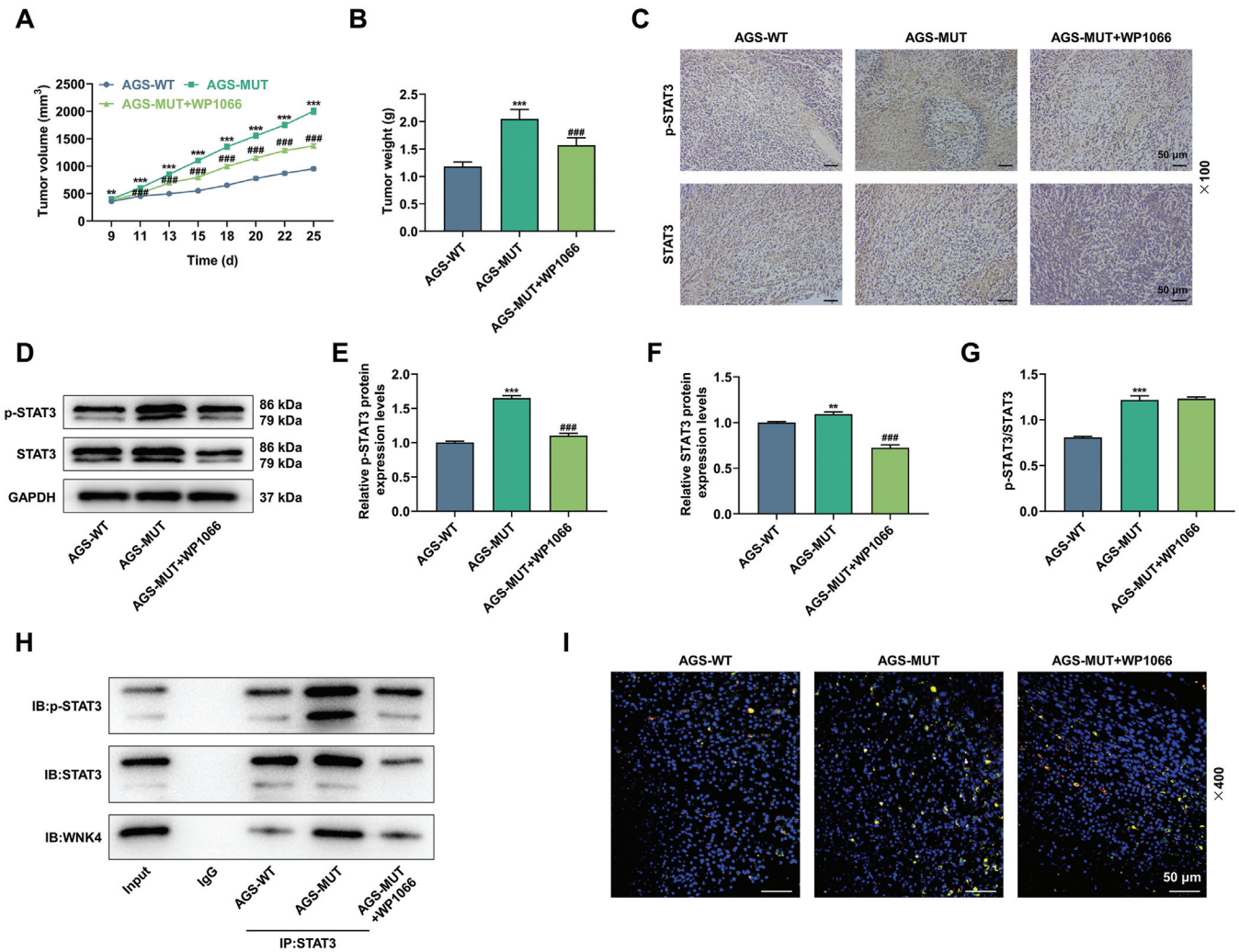

Fig. 3. STAT3 inhibitor reversed the effects of WNK4 mutation on accelerating tumor growth and activating STAT3 in tumor-bearing mice. **A-I.** Tumor-bearing mice were constructed with WT or MUT AGS cells, and some mice were injected with 40 mg/kg STAT3 inhibitor WP1066 for 21 days (AGS-WT, AGS-MUT, and AGS-MUT+WP1066 groups). **A.** Tumor volume within 25 days post-injection. **B.** Tumor weight on day 25 post-injection. **C.** Immunohistochemistry results for p-STAT3 and STAT3 location in tumors. **D-G.** Western blot data showed expressions of p-STAT3 and STAT3 in tumors, with GAPDH as the internal reference, and the value of p-STAT3/STAT3 was calculated. **H.** Co-immunoprecipitation assay results revealed the interaction between WNK4 and STAT3 in tumors. **I.** Immunofluorescence co-localization of WNK4 and STAT3 in tumors. $^{**}p<0.01$, $^{***}p<0.001$ vs. AGS-WT; $^{###}p<0.001$ vs. AGS-MUT. IB, immunoblotting, Input, positive control; IP, immunoprecipitation.

with the upregulated trend of the p-STAT3/STAT3 value in all the above processes. Furthermore, we identified the combination of WNK4 with STAT3 by co-immunoprecipitation and immunofluorescence co-localization in tumors, which was further confirmed by the finding that STAT3 inhibitor reversed the effects of WNK4 mutation in tumors. These findings contributed to understanding GC pathogenesis and provided potential molecular targets for GC clinical treatment.

WNK4, on chromosome 17 in humans, was initially identified in 2001 when Richard Lifton's team discovered mutations that cause human hypertension (Wilson et al., 2001). In the context of *WNK1* and *WNK4* mutations in pseudoaldosteronism type II, new *WNK4* mutations have been discovered, including E562K, D564A, D564H, Q565E, R1185C, P561L, D564N, and D561A (Wilson et al., 2001; Golbang et al., 2005; Gong et al., 2008; Chiga et al., 2011; Sakoh et al., 2019). An earlier cancer study showed that WNK3 and WNK4 mutations occur in leukemia stem cells (Mabrey et al., 2018). Another research reported that WNK2 mutation is present in patients with gastric cardia adenocarcinoma or gastric noncardia adenocarcinoma (Hu et al., 2016). However, to the best of our knowledge, to date, there is no report on *WNK4* mutation in GC. We constructed a new *WNK4* mutation with a deleted guanine at position 1816 via the CRISPR/Cas9 method and stably transfected it into GC cells. Here, we indicated that *WNK4* mutation strengthened the *in vitro* survival ability of GC cells. In addition, we also clarified that *WNK4* mutation weakened the sensitivity of GC cells to 5-FU and CDDP. Collectively, WNK4 may function as an antioncogene in GC development, and its mutation may promote GC cell growth and resistance.

With dual functions of signal transduction and transcriptional activation, STAT3 is a transcription factor widely expressed in normal tissues and can regulate intracellular biological behaviors through the Janus Kinase (JAK)/STAT signaling pathway (Zhang et al., 2023). Through binding growth factors or cytokines to their corresponding receptors or JAK, STAT3 phosphorylation is induced; the phosphorylated STAT3 dimer recognizes and binds to specific DNA binding elements, thus initiating the transcription of specific downstream genes and generating the corresponding biological effects (Menon et al., 2021). *STAT3* is defined as an oncogene owing to its aberrant activation in most human tumors (Alqahtani et al., 2023). In recent years, it has been found that interleukin-6/8/11 (IL-6/8/11) can promote the growth and invasion of GC through the JAK-STAT pathway (Li et al., 2016; Zhao et al., 2016; Wang et al., 2018). As for the resistance of tumor cells to chemotherapeutic agents, the sustained activation of STAT3 also plays a crucial role, and inhibiting STAT3 has been regarded as an effective treatment means (Wang and Ma, 2022). Of note, somatic mutations lead to the sustained activation of STAT3. For instance, somatic epidermal growth factor receptor (EGFR)-activating mutations can activate the STAT3 pathway by upregulating IL-6 in lung cancer (Yang et al., 2019). Similarly, GC progression requires Kras oncogene mutation that acts synergistically with STAT3 activation (Thiem et al., 2016). Costa et al. found that silencing protein kinase WNK2 activates JNK and promotes gliomas (Margarida Costa et al., 2014). Due to the close association of JNK with STAT3, we hypothesized that WNK4 might act as an antioncogene in tumorigenesis through the activation of the STAT3 pathway. Accordingly, we examined the activation of STAT3 phosphorylation in GC cells in the presence of WNK4 mutation, and the upregulation of p-STAT3/STAT3 was identified in GC cells with/without drug treatment, which preliminarily evidenced our hypothesis.

In order to demonstrate the in-depth relationship between STAT3 and WNK4, we further performed *in vivo* trials. We unveiled that WNK4 mutation accelerated tumor growth in mice models, implying that WNK4 acted as an antioncogene in GC. Besides, WNK4 mutation increased the expression of p-STAT3 and STAT3 and their ratio in tumors. STAT3 inhibitor WP1066 reversed the effects of WNK4 mutation on tumor growth and STAT3 activation, mirroring that STAT3 mediated WNK4 function in GC. All mammalian WNKs have a short amino-terminal domain, a highly conserved serine/threonine kinase domain, a self-repressor domain, and at least two helix domains (Murillo-de-Ozores et al., 2021). Helix domains at the carboxyl terminus of WNK kinase are involved in the binding of other proteins. WNK1 partially co-localizes with the UV radiation resistance-associated gene (UVRAG), which is inhibited when autophagy is stimulated in cells, and the loss of WNK1 also alters the cellular distribution of UVRAG (Kankanamalage et al., 2017). WNK3 stimulates glioma invasion by co-localizing and co-immunoprecipitation with sodium-potassium-chloride cotransporter isoform-1 (NKCC1) to regulate cell volume (Haas et al., 2011). Consistently, we observed co-immunoprecipitation and co-localizing of WNK4 and STAT3 in tumors, which was enhanced by WNK4 mutation. Importantly, the combination between WNK4 and STAT3 was further supported by the weakened co-immunoprecipitation and co-localization with WP1066.

To sum up, this study reveals a novel mutation of WNK4 in GC, which impacts both the natural and drug-treated growth of GC cells or tumors through activating STAT3. These findings provide a new genetic model for preclinical research to identify new therapeutic targets or to clarify the specific role of WNK4 mutation in the pathogenesis and development of GC.

Acknowledgements. Not applicable

Data availability. The analyzed data sets generated during the study are available from the corresponding author upon reasonable request.

Conflict of interest. The authors declare that there is no conflict of interest.

Funding. Not applicable.

References

Alqahtani T., Kumarasamy V., Alghamdi S.S., Suliman R.S., Bin Saleh K., Alrashed M.A., Aldhaeefi M. and Sun D. (2023). Adefovir dipivoxil as a therapeutic candidate for medullary thyroid carcinoma: Targeting ret and stat3 proto-oncogenes. Cancers (Basel.) 15, 2163.

Arreola-Peralta L.D., Altamirano-Reyna F., Galindo-González D.M., Solis-Anguiano J.G., Lacivita E., Leopoldo M. and Terrón J.A. (2018). Potentiation of capsaicin-induced neurogenic inflammation by 5-ht7 receptors in the rat hind paw: Involvement of calcitonin gen-related peptide. Peptides. 105, 1-6.

Chen Y.L., Wang C.Y., Fang J.H. and Hsu H.P. (2021). Serine/threonine-protein kinase 24 is an inhibitor of gastric cancer metastasis through suppressing *CDH1* gene and enhancing stemness. Am. J. Cancer Res. 11, 4277-4293.

Chiga M., Rafiqi F.H., Alessi D.R., Sohara E., Ohta A., Rai T., Sasaki S. and Uchida S. (2011). Phenotypes of pseudohypoaldosteronism type II caused by the WNK4 D561A missense mutation are dependent on the WNK-OSR1/SPAK kinase cascade. J. Cell Sci. 124, 1391-1395.

Golbang A.P., Murthy M., Hamad A., Liu C.H., Cope G., Van't Hoff W., Cuthbert A. and O'Shaughnessy K.M. (2005). A new kindred with pseudohypoaldosteronism type ii and a novel mutation (564D>H) in the acidic motif of the WNK4 gene. Hypertension 46, 295-300.

Gong H., Tang Z., Yang Y., Sun L., Zhang W., Wang W., Cui B. and Ning G. (2008). A patient with pseudohypoaldosteronism type II caused by a novel mutation in WNK4 gene. Endocrine 33, 230-234.

Haas B.R., Cuddapah V.A., Watkins S., Rohn K.J., Dy T.E. and Sontheimer H. (2011). With-no-lysine kinase 3 (WNK3) stimulates glioma invasion by regulating cell volume. Am. J. Physiol. Cell Physiol. 301, C1150-C1160.

Hou C.-Y., Ma C.-Y. and Yuh C.-H. (2022). WNK1 kinase signaling in metastasis and angiogenesis. Cell Signal. 96, 110371.

Hu N., Kadota M., Liu H., Abnet C.C., Su H., Wu H., Freedman N.D., Yang H.H., Wang C., Yan C., Wang L., Gere S., Hutchinson A., Song G., Wang Y., Ding T., Qiao Y.-L., Koshiol J., Dawsey S.M., Giffen C., Goldstein A.M., Taylor P.R. and Lee M.P. (2016). Genomic landscape of somatic alterations in esophageal squamous cell carcinoma and gastric cancer. Cancer Res. 76, 1714-1723.

Kabwe J.C., Sawada H., Mitani Y., Oshita H., Tsuboya N., Zhang E., Maruyama J., Miyasaka Y., Ko H., Oya K., Ito H., Yodoya N., Otsuki S., Ohashi H., Okamoto R., Dohi K., Nishimura Y., Mashimo T., Hirayama M. and Maruyama K. (2022). CRISPR-mediated Bmpr2 point mutation exacerbates late pulmonary vasculopathy and reduces survival in rats with experimental pulmonary hypertension. Respir. Res. 23, 87.

Kang B.W. and Chau I. (2020). Molecular target: Pan-AKT in gastric cancer. ESMO Open 5, e000728.

Kankanamalage S.G., Lee A.Y., Wichaidit C., Lorente-Rodriguez A., Shah A.M., Stippec S., Whitehurst A.W. and Cobb M.H. (2017). WNK1 is an unexpected autophagy inhibitor. Autophagy 13, 969-970.

Kankanamalage S.G., Karra A.S. and Cobb M.H. (2018). WNK pathways in cancer signaling networks. Cell Commun. Signal. 16, 72.

Kannaiyan R. and Mahadevan D. (2018). A comprehensive review of protein kinase inhibitors for cancer therapy. Expert. Rev. Anticanc. 18, 1249-1270.

Li W., Lin S., Li W., Wang W., Li X. and Xu D. (2016). IL-8 interacts with metadherin promoting proliferation and migration in gastric cancer. Biochem. Bioph. Res. Co. 478, 1330-1337.

Mabrey F.L., Chien S.S., Martins T.S., Annis J., Sekizaki T.S., Dai J., Beckman R.A., Loeb L.A., Carson A., Patay B., Blau C.A., Oehler V.G., Celik S.S., Lee S.-I., Monnat R.J., Abkowitz J.L., Appelbaum F.R., Estey E.H. and Becker P.S. (2018). High throughput drug screening of leukemia stem cells reveals resistance to standard therapies and sensitivity to other agents in acute myeloid leukemia. Blood 132, 180-180.

Margarida Costa A., Pinto F., Martinho O., José Oliveira M., Jordan P. and Manuel Reis R. (2014). Silencing of WNK2 is associated with upregulation of MMP2 and JNK in gliomas. 6, 1422-1434.

Menon P.R., Doudin A., Gregus A., Wirths O., Staab J. and Meyer T. (2021). The anti-parallel dimer binding interface in STAT3 transcription factor is required for the inactivation of cytokine-mediated signal transduction. Biochim. Biophys. Acta Mol. Cell Res. 1868, 119118.

Morgan E., Arnold M., Camargo M.C., Gini A., Kunzmann A.T., Matsuda T., Meheus F., Verhoeven R.H.A., Vignat J., Laversanne M., Ferlay J. and Soerjomataram I. (2022). The current and future incidence and mortality of gastric cancer in 185 countries, 2020-40: A population-based modelling study. EClinicalMedicine 47, 101404.

Murillo-de-Ozores A.R., Rodríguez-Gama A., Bazúa-Valenti S., Leyva-Ríos K., Vázquez N., Pacheco-Álvarez D., De La Rosa-Velázquez I.A., Wengi A., Stone K.L., Zhang J., Loffing J., Lifton R.P., Yang C.-L., Ellison D.H., Gamba G. and Castañeda-Bueno M. (2018). C-terminally truncated, kidney-specific variants of the wnk4 kinase lack several sites that regulate its activity. J. Biol. Chem. 293, 12209-12221.

Murillo-de-Ozores A.R., Rodríguez-Gama A., Carbajal-Contreras H., Gamba G. and Castañeda-Bueno M. (2021). WNK4 kinase: From structure to physiology. Am. J. Physiol. Renal Physiol. 320, F378-f403.

Najar M.A., Modi P.K., Ramesh P., Sidransky D., Gowda H., Prasad T.S.K. and Chatterjee A. (2021). Molecular profiling associated with calcium/calmodulin-dependent protein kinase kinase 2 (CAMKK2)-mediated carcinogenesis in gastric cancer. J. Proteome Res. 20, 2687-2703.

Patel T.H. and Cecchini M. (2020). Targeted therapies in advanced gastric cancer. Curr. Treat. Options Oncol. 21, 70.

Qiao Y., Li T., Zheng S. and Wang H. (2018). The Hippo pathway as a drug target in gastric cancer. Cancer Lett. 420, 14-25.

Rafael C., Soukaseum C., Baudrie V., Frère P. and Hadchouel J. (2018). Consequences of spak inactivation on hyperkalemic hypertension caused by WNK1 mutations: Evidence for differential roles of WNK1 and WNK4. Sci. Rep. 8, 3249.

Sakoh T., Sekine A., Mori T., Mizuno H., Kawada M., Hiramatsu R., Hasegawa E., Hayami N., Yamanouchi M., Suwabe T., Sawa N., Ubara Y., Fujimaru T., Sohara E., Shinichi U., Hoshino J. and Takaichi K. (2019). A familial case of pseudohypoaldosteronism type ii (PHA22) with a novel mutation (D564N) in the acidic motif in WNK4. 7, e705.

Smyth E.C., Nilsson M., Grabsch H.I., van Grieken N.C.T. and Lordick F. (2020). Gastric cancer. The Lancet 396, 635-648.

Sung H., Ferlay J., Siegel R.L., Laversanne M., Soerjomataram I., Jemal A. and Bray F. (2021). Global cancer statistics 2020: GLOBOCAN estimates of incidence and mortality worldwide for 36 cancers in 185 countries. CA Cancer. J. Clin. 71, 209-249.

Thiem S., Eissmann M.F., Elzer J., Jonas A., Putoczki T.L., Poh A.,

Nguyen P., Preaudet A., Flanagan D., Vincan E., Waring P., Buchert M., Jarnicki A. and Ernst M. (2016). Stomach-specific activation of oncogenic KRAS and STAT3-dependent inflammation cooperatively promote gastric tumorigenesis in a preclinical model. Cancer Res. 76, 2277-2287.

Wang X., Che X., Liu C., Fan Y., Bai M., Hou K., Shi X., Zhang X., Liu B., Zheng C., Liu Y. and Qu X. (2018). Cancer-associated fibroblasts-stimulated interleukin-11 promotes metastasis of gastric cancer cells mediated by upregulation of MUC1. Exp. Cell Res. 368, 184-193.

Wang B., Guan G. and Zhao D. (2020). Silence of FAM83H-AS1 promotes chemosensitivity of gastric cancer through Wnt/β-catenin signaling pathway. Biomed. Pharmacother. 125, 109961.

Wang H. and Ma Y. (2022). β-Elemene alleviates cisplatin resistance in oral squamous cell carcinoma cell via inhibiting JAK2/STAT3 pathway *in vitro* and *in vivo*. Cancer Cell Int. 22, 244.

Wang Y., Guo Z., Tian Y., Cong L., Zheng Y., Wu Z., Shan G., Xia Y., Zhu Y., Li X. and Song Y. (2023). MAPK1 promotes the metastasis and invasion of gastric cancer as a bidirectional transcription factor. BMC Cancer 23, 959.

Wei Z.W., Xia G.K., Wu Y., Chen W., Xiang Z., Schwarz R.E., Brekken R.A., Awasthi N., He Y.L. and Zhang C.H. (2015). CXCLl1 promotes tumor growth through VEGF pathway activation and is associated with inferior survival in gastric cancer. Cancer Lett. 359, 335-343.

Wilson F.H., Disse-Nicodème S., Choate K.A., Ishikawa K., Nelson-Williams C., Desitter I., Gunel M., Milford D.V., Lipkin G.W., Achard J.-M., Feely M.P., Dussol B., Berland Y., Unwin R.J., Mayan H., Simon D.B., Farfel Z., Jeunemaitre X. and Lifton R.P. (2001). Human hypertension caused by mutations in WNK kinases. Science 293, 1107-1112.

Xiu M., Li L., Li Y. and Gao Y. (2022). An update regarding the role of WNK kinases in cancer. Cell Death Dis. 13, 795.

Yang Y., Wang W., Chang H., Han Z., Yu X. and Zhang T. (2019). Reciprocal regulation of miR-206 and IL-6/STAT3 pathway mediates IL6-induced gefitinib resistance in EGFR-mutant lung cancer cells. J. Cell Mol. Med. 23, 7331-7341.

Yoon H.J., Kim G.-C., Oh S., Kim H., Kim Y.K., Lee Y., Kim M.S., Kwon G., Ok Y.-S., Kwon H.-K. and Kim H.S. (2022). Wnk3 inhibition elicits antitumor immunity by suppressing PD-l1 expression on tumor cells and activating T-cell function. Exp. Mol. Med. 54, 1913-1926.

Yu L.J., Wang B., Parobchak N., Roche N. and Rosen T. (2015). STAT3 cooperates with the non-canonical NK-κB signaling to regulate pro-labor genes in the human placenta. Placenta 36, 581-586.

Zhang K., Dong W., Li J., Gong Z., Liu W., He S., Zou H., Song R., Liu G. and Liu Z. (2022). Honokiol antagonizes cadmium-induced nephrotoxicity in quail by alleviating autophagy dysfunction, apoptosis and mitochondrial UPR inhibition with its antioxidant properties. Life (Basel) 12, 1574.

Zhang Z., Fan K., Meng J., Nie D., Zhao Z. and Han Z. (2023). Deoxynivalenol hijacks the pathway of janus kinase 2/signal transducers and activators of transcription 3 (JAK2/STAT-3) to drive caspase-3-mediated apoptosis in intestinal porcine epithelial cells. Sci. Total Environ. 864, 161058.

Zhao G., Zhu G., Huang Y., Zheng W., Hua J., Yang S., Zhuang J. and Ye J. (2016). IL-6 mediates the signal pathway of JAK-STAT3-VEGF-C promoting growth, invasion and lymphangiogenesis in gastric cancer. Oncol. Rep. 35, 1787-1795.

Zhao Z., Fang Q., Wei L., Lin J., Su R. and Li N. (2023). Autophagy-related gene *CXCR4* is a potential predictor of prognosis and immunotherapy response for gastric cancer. Discov. Med. 35, 1190-1201.

Zheng Y., Li Z., Wang Y., Chen W., Lin Y., Guo J. and Ye G. (2023). CircRNA: A new class of targets for gastric cancer drug resistance therapy. Pathol. Oncol. Res. 29, 1611033.

Zhou X., Ren Y., Liu A., Han L., Zhang K., Li S., Li P., Li P., Kang C., Wang X. and Zhang L. (2014). Stat3 inhibitor wp1066 attenuates mirna-21 to suppress human oral squamous cell carcinoma growth *in vitro* and *in vivo*. Oncol. Rep. 31, 2173-2180.

Zuo Y., Lv Y., Qian X., Wang S., Chen Z., Jiang Q., Cao C. and Song Y. (2018). Inhibition of HHIP promoter methylation suppresses human gastric cancer cell proliferation and migration. Cell Physiol. Biochem. 45, 1840-1850.

Accepted September 9, 2024